Competition between the Rad50 complex and the Ku heterodimer reveals a role for Exo1 in processing double-strand break, but not telomeres

Kazunori Tomita[1], Akira Matsuura[2], Thomas Caspari[3], Antony M. Carr[3], Yufuko Akamatsu[4], Hiroshi Iwasaki[4], Ken-ichi Mizuno[5], Kunihiro Ohta[5], Masahiro Uritani[1], Takashi Ushimaru[6], Koichi Yoshinaga[1], and Masaru Ueno[7]

[1]Department of Chemistry, [6]Department of Biology, Shizuoka University, 836 OYA, Shizuoka, 422-8529 JAPAN

[2]Department of Geriatric Research, National Institute for Longevity Science, 36-3 Gengo, Morioka, Obu, Aichi, 474-8522 JAPAN

[3] Genome Damage and Stability Centre, University of Sussex, Brighton BN19RQ, UK.

[4] Graduate School of Integrated Science, Yokohama City University

1-7-29 Suehirocho, Tsurumi-ku, Yokohama, Kanagawa, 230-0045 JAPAN

[5] Genetic Dynamics Research Unit-Laboratory, RIKEN Institute, 2-1, Hirosawa , Wako,

Saitama, 351-0198 JAPAN

[7] Corresponding author.

e-mail: scmueno@ipc.shizuoka.ac.jp

Running head: Function of Rad50 and Ku at DSB and Telomere ends

Telephone: +81-54-238-4762

Fax: +81-54-237-3384

Abstract

The Mre11-Rad50-Nbs1(Xrs2) complex and the Ku70-Ku80 heterodimer are thought to compete with each other for binding to DNA ends. To investigate the mechanism underlying this competition, we analyzed both DNA damage sensitivity and telomere overhangs in *S. pombe rad50-d*, *rad50-d pku70-d, rad50-d exo1-d,* and *pku70-d rad50-d exo1-d* cells. We found that *rad50 exo1* double mutants are more MMS sensitive than the respective single mutants. The MMS sensitivity of *rad50-d* cells was suppressed by concomitant deletion of *pku70*$^{+}$. However, the MMS sensitivity of the *rad50 exo1* double mutant was not suppressed by deletion of *pku70*$^{+}$. The G-rich overhang at telomere ends in *taz1-d* cells disappeared upon deletion of *rad50*$^{+}$, but the overhang reappeared following concomitant deletion of *pku70*$^{+}$. Our data suggest that the Rad50 complex can process DSB ends and telomere ends in the presence of Ku heterodimer. However, Ku heterodimer inhibits processing of DSB ends and telomere ends by alternative nucleases in the absence of the Rad50-Rad32 protein complex. While we have identified Exo1 as the alternative nuclease targeting DNA break sites, the identity of the nuclease acting on the telomere ends remains

elusive.

(**Introduction**)

While a DNA double-strand break within a chromosome must be repaired to prevent cell death, a chromosome end is not recognized as DNA damage, and is protected from the action of repair enzymes. It was therefore surprising when it was shown that several DNA repair proteins, including Mre11 and Ku, are involved in both DNA DSB repair and telomere maintenance (23, 24). Telomeres, the natural DNA ends of eukaryotic chromosomes (9), are stable and do not fuse with other chromosome ends. In order that telomeres can be treated as specialized DNA structures and not as DNA damage, they are composed of repetitive DNA elements and associated with specialized proteins including human TRF1 and TRF2, *S. pombe* Taz1p or *S. cerevisiae* Rap1 (4, 10, 11, 31, 62). Disruption of telomere architecture caused by the deletion of *S. pombe taz1*$^{+}$, for example, leads to massive telomere elongation and Ku-dependent end-to-end fusions (11, 20).

In eukaryotic cells, DSBs are mainly repaired either by homologous recombination (HR) or non-homologous end joining (NHEJ) (12-14, 23, 24, 27). In the yeast *S. cerevisiae*, DNA DSBs are predominantly repaired by HR, which requires

genes of the Rad52 epistasis group (50). The first step of HR is ssDNA end resection in a 5' to 3' direction to form long 3' single-stranded tails (53). Although the Mre11-Rad50-Xrs2 (MRX) complex is thought to participate in this step (29), under *in vitro* conditions, Mre11 exhibits exonuclease activity of the opposite polarity, namely 3' to 5' exonuclease activity against both ssDNA and dsDNA (21, 40, 51, 61). Mre11 aso displays a single-stranded DNA (ssDNA) endonuclease activity. Consistent with this observation, mutants in the Mre11 nuclease motif are not as ionized radiation (IR)-sensitive as would be expected for mutants in an enzyme required for end processing (40). Furthermore, the observation that overexpression of exonuclease I (Exo1) partially suppress the DNA-damage sensitivity of Mre11 mutants (30, 41, 58) suggests that Exo1 acts redundantly with Mre11 in end-processing.

In contrast to the situation in yeast, the major mechanism for the repair of radiation-induced DSBs in higher eukaryotes is NHEJ. The Ku70-Ku80 heterodimer, DNA-PKcs and a DNA ligaseIV-Xrcc4 complex are all required for this process (19, 22, 63). NHEJ is not a major mechanism of DNA repair in *S. cerevisiae*, but yeast Ku70, Ku80 and Lig4 are essential for the repair of plasmid DSBs following transformation of

linearized plasmid into cells (38, 59). In *S. cerevisiae*, the IR sensitivity of *mre11* null mutants is partially suppressed by loss of *YKU70* (7). Furthermore, the rate of 5' to 3' degradation of HO-induced DSBs is decreased by deletion of *MRE11* and increased by deletion of *YKU70.* These data have led to a model in which the Ku pathway competes with 5' to 3' exonuclease at DNA ends (29). However, it is unclear which nuclease is competing with Yku70. In contrast to IR sensitivity, the MMS sensitivity of *mre11* null mutants is not suppressed by the loss of *YKU70* (38). The *yku70* single mutant is not MMS sensitive, indicating that Ku heterodimers play no role in the repair of MMS-induced DNA damage (52, 60).

Ku has also been characterized in the fission yeast *S. pombe.* The Ku heterodimer is required for NHEJ of transformed linear plasmids and for the maintenance of correct telomere length (3, 32, 39). In contrast to *S. cerevisiae* Yku70, fission yeast Ku70 does not accumulate in telomeric foci. Moreover, deletion of the fission yeast gene encoding Ku70 (*pku70*$^{+}$) does not overcome telomere silencing, indicating that the function of Ku at telomere ends is not fully conserved between fission and budding yeasts (6, 32, 35). *S. pombe* Rad50 and Rad32 (a homologue of *S.*

cerevisiae Mre11) are both involved in telomere length maintenance and DNA repair (25, 32, 56, 65, 66), but, in contrast to their homologues in *S. cerevisiae*, they are not required for the delay to S phase progression that occurs upon treatment with hydroxylurea (HU) or methylmethane sulfonate (MMS) (25, 33). Although the cellular function of the Rad32-Rad50 protein complex is still not understood, recent data suggest that during DNA replication the complex is required to cleave hairpin structures, which would be produced from palindromic sequences during lagging strand DNA synthesis (18).

The Rad50 complex is required for both HR and NHEJ in *S. cerevisiae* (23), making it difficult to study the exact roles of the Rad50 complex and Ku heterodimer in HR repair separately from their effects on NHEJ. However, it is possible to study the role of the *S. pombe* Rad50 complex in HR repair because the *S. pombe* Rad50 complex is not required for NHEJ (32). We report here an investigation of the different roles of the Rad50-Rad32 protein complex and the Ku heterodimer at DSB ends generated in response to DNA damage and at telomere ends in *taz1-d* cells. Our data suggest that both types of DNA ends are mainly processed in a manner dependent on the

Rad32-Rad50 complex. We also provide evidence suggesting that, in the absence of the Rad32-Rad50 complex (which appears to play the primary role), the Ku70/80 heterodimer has to be removed from either type of DNA end to provide access for alternative end-processing pathways. Our data strongly indicate that exonuclease 1 (Exo1) is one of these alternative nucleases. Interestingly, Exo1 seems to act only on DNA ends generated by DNA damage and not on telomeric DNA ends, which are targeted by another as yet unidentified nuclease.

MATERIALS AND METHODS

Growth medium. *S. pombe* cells were grown in YPAD medium (1% yeast extract, 2% polypeptone, 2% glucose, 20 μ g/ml adenine), YEA medium (0.5% yeast extract, 3% glucose, 20 μ g/ml adenine) or EMM medium with required supplements (42).

Strain construction. The *rad50*$^+$ gene was disrupted by replacing the region between the first *Hind*III restriction site and second *Hind*III site (nucleotide positions 529-1158 relative to initiation codon) with either the *ura4*$^+$or the *LEU2*$^+$ gene. Standard methods were used to create the disrupted constructs, and linear fragments were transformed into a wild-type strain (JY741) (42). *rad32-d* , *trt1-d* and *taz1-d* cells were constructed by insertion of the *ura4*$^+$ or *LEU2*$^+$ cassette into the *Hind*III , *Bgl*II and *Pst*I sites, respectively. *pku70-d*, *pku80-d* and *lig4-d* cells were constructed by insertion of the *LEU2*$^+$ cassette into the *Eco*RV, *Eco*RV and *Nco*I sites respectively. To construct *pku70:: LEU2:: ade6*$^+$ cells, the *ade6*$^+$cassette was inserted into the *Eco*RV site in the *LEU2* gene in the *pku70:: LEU2* disruption fragment. *rad50 taz1* and *rad50 pku70* double mutants were constructed by transformation of *taz1* and *pku70* mutants

with the *rad50* disruption fragment. The *rad32 taz1* double mutant was constructed by transforming *rad32-d* cells with a *taz1* disruption fragment. *rhp51-d* cells were constructed by insertion of the *ura4*$^+$cassette in the *Nhe*I site of the *rhp51* gene. To tag Rad32 with the Myc epitope at the C-terminus, we amplified the *rad32*$^+$ ORF by PCR with a primer set of Rad32T (5'-GCATACCCGGGATCATCTAAAATTTCGTCATCC-3') and Rad32B (5'-GCATACCCGGGATCATCTAAAATTTCGTCATCC-3'), using wild-type genomic DNA as a template. The *Sma*I cut PCR fragment was then cloned into *Sma*I cut pFA6a-13Myc-kanMX6, which contained 13 copies of Myc epitope and a kanMX6 marker. pFA6a-13Myc-kanMX6 was provided by John R. Pringle (University of North Carolina) (1). The resulting plasmid was linearized with *Bsa*BI, and used for transformation. Other double and triple mutants were constructed by genetic crosses.

In-gel hybridization. In-gel hybridization analysis was performed according to the protocol previously published (16) using a G-rich probe: 5'-GATCG

GGTTACA A GGTTACG T GGTTACA CG-3' and a C-rich probe: 5'-CG TGTAACC A CGTAACC T TGTAACC CGATC-3'. A plasmid containing the telomere-repeat sequence derived from pNSU70 (46), was used as a dsDNA and ssDNA control. For the dsDNA control, about 5 ng of *Apa*I-digested plasmid containing 300–bp-long telomere DNA was loaded. For the ssDNA control, the same amount of heat-denatured *Apa*I-digested plasmid was loaded. One microgram of genomic DNA was digested with *Eco*RI and electrophoresed on a 0.5% agarose gel in 0.5×TAE buffer with 0.01 mg/ml ethidium bromide. The gel was vacuum dried at 45°C until it become thin and warm (about 45 min). Single-stranded telomeric DNA probe was labeled with [γ-^{32}P] ATP (Amersham Pharmacia Biotech) using T4 polynucleotide kinase. An AlkPhos DirectTM kit was used for hybridization. The gel was pre-hybridized in hybridization buffer at 37°C for 15min, and then 10 pmol of probe was added and the incubation was continued at 37°C overnight. The gel was washed with primary wash buffer at 37°C for 2×10 min and then washed with secondary wash buffer at room temprature for 3×5 min (AlkPhos DirectTM, Amersham Pharmacia Biotech). The gel was dried on the Whatman paper and exposed to X-ray film for about 2 days. To detect

the double-stranded telomere DNA, the gel was treated with denaturing solution (0.5 M NaOH, 150 mM NaCl) for 25 min at room temperature, and was treated with neutralizing solution (0.5 M Tris-HCl pH 8.0 150 mM NaCl) and reprobed with the same probe by in-gel hybridization.

DNA damage sensitivity assay. Clonogenic cell survival after MMS treatment was determined as described previously (38). Logarithmically growing cells were plated directly onto solid medium containing 0.002% MMS. Colonies formed on the control and MMS-containing plates were counted after 4 days of incubation at 30 °C, and the surviving fraction was calculated. For the spot assay, 4 μl of 10-fold dilutions of log-phase cells ($0.5x10^7$ cells/ml) were spotted onto a YEA (a 2% gar) plate or YEA plate containing the indicated concentration of MMS. For IR survival, logarithmically growing cells were irradiated using a ^{137}Cs source at a dose rate of 12.5 Gy/min. For UV survival, a germicidal lamp (FUNA-UV-LINKER, FS-800) was used at a dose rate of 50-200 $J/m^2/min$. Irradiated cells and unirradiated cells were plated on YPAD medium plates and incubated at 30 °C for 4 days. All experiments were repeated at least twice.

Indirect immunofluorescence microscopy. Indirect immunofluorescence microscopy was performed according to the protocol previously published in (8) with the following change: Anti-hRad51 (Santa Cruz H-92) was diluted 1:100. To determine the percentage of cells showing nuclear foci, we visually scored 1000 cells for each sample.

Immunoprecipitation. For immunoprecipitation, IgG-conjugated magnetic beads were produced with Tosylactivated Dynabeads M-280 (DYNAL) and Mouse IgG according to the manufacturer's instructions. 20 μl of Dynabeads were added to 12mg of total proteins in 400 μl of buffer (50mM HEPES/KOH pH7.5, 140mM NaCl, 300mM $(NH_2)_2SO4$, 1mM EDTA, 1% (v/v) Triton X-100, 0.1% (w/v) sodium deoxycholate, 0.01% (w/v) BSA, protease inhibitor cocktail (Roche), 1mM PMSF and 1mM DTT). This mixture was incubated for 2 hr at 4 °C. After extensive washing, the beads were suspended in 50 μl of sodium dodecyl sulfate (SDS)-sample buffer. 10 μl of the suspension was analyzed on Western Blot. The anti-Myc-Tag 9B11 antibody (Cell Signaling) and anti-Protein A antibody (Sigma) were used for detection of proteins.

Chromatin Immunoprecipitation. The ChIP assay described by Takahashi

et al. (55) was adopted with modification. Cells grown in 100 ml of YPAD culture at 30 °C were fixed with formaldehyde. For immunoprecipitation, anti-Myc-Tag 9B11 antibody (Cell Signaling) and protein G coated dynabeads (DYNAL) were used. Immunoprecipitated DNA was extracted and suspended in TE buffer (10mM Tris-HCl, 1 mM EDTA). PCR reactions used the following primers to amplify the telomeric DNA (TOP 5'-CGGCTGACGGGTGGGGCCCAATA-3' BOTTOM 5'-GTGTGGAATTGAGTATGGTGAA-3') or the *ade6*$^{+}$ DNA (TOP 5'-AGGTATAACGACAACAAACGTTGC -3' BOTTOM 5'-CAAGGCATCAGTGTTAATATGCTC -3')

RESULTS

The DNA damage sensitivity of *rad50-d* cells is suppressed by deletion of *pku70*$^+$. The Rad50-Mre11-Nbs1(Xrs2) complex and the Ku heterodimer are thought to compete with each other for binding to DSB ends (29). To investigate the mechanism underlying this competition, we analyzed the DNA damage sensitivities of *rad50-d* cells and *rad50 pku70* double mutants in *S. pombe*. We found that the γ-ray sensitivity of *rad50-d* cells was suppressed by deletion of *pku70*$^+$ (Fig. 1A). By analogy to the mechanism proposed for *S. cerevisiae*, where the IR sensitivity of *mre11* null mutants is partially suppressed by the loss of *YKU70* (7), our results suggest that deletion of *pku70*$^+$ in *S. pombe* cells lacking a functional Rad50-Rad32 protein complex improves the efficiency of HR repair by enhancing the ability to process DSB ends. In *S. cerevisiae*, the MMS sensitivity of *mre11* mutants is not suppressed by the loss of *yku70* (38). However, we found that the MMS, UV and HU sensitivities of *rad50-d* cells were suppressed by concomitant deletion of *pku70*$^+$ (Figs. 1B-D). These results strongly suggest that *S. pombe* Ku70 plays an important role in the repair of MMS, UV and HU-induced DNA damage, probably by inhibiting HR repair in the absence of the

Rad50 complex. As *rad50*$^+$ is epistatic to *rad32*$^+$ for DNA damage sensitivity, we examined whether *rad50-d* cells and *rad32-d* cells display the same phenotype with respect to the suppression of DNA damage sensitivity. Spot assays revealed that deletion of *pku70*$^+$ suppressed the sensitivity of both *rad50-d* and *rad32-d* cells to MMS and HU (data not shown).

Because the function of Rad50 is thought to be in DNA damage processing, upstream of Rad51, the suppression of DNA damage sensitivity presumably reflects the enhancement of DSB ends processing. In this case, suppression should be limited to the early stages of HR. We therefore asked whether the MMS sensitivity of *rhp51-d* cells, which are defective in later steps in HR (43), is also suppressed by the deletion of *pku70*$^+$. The survival of *rhp51-d* cells at 0.002% MMS (0.1% ± 0.01) was almost same as that of *rhp51 pku70* double mutants (0.1% ± 0.01) (Fig. 2). These results indicate that the suppressions of DNA damage sensitivity occurs at an early stage in HR, probably before strand invasion, which requires Rad51 (Rhp51).

Similarly, Ku70/Ku80 is thought to function at an early stage of NHEJ and Lig4 at a later stage (3, 39). We investigated whether the DNA damage sensitivity of

rad50-d cells was suppressed by the deletion of either *pku80*$^{+}$ or *lig4*$^{+}$. The MMS sensitivity of *rad50-d* cells was suppressed by concomitant deletion of *pku80*$^{+}$, but was not significantly suppressed by concomitant the deletion of *lig4*$^{+}$ (Fig. 2). These results indicate that the DNA binding of the Ku70/80 heterodimer plays an important role in the suppression of DNA damage sensitivity.

Evidence that Exo1 resects DNA double-strand break ends in the absence of Rad50 and Ku70. The data presented above suggest that the Ku heterodimer represses a repair function early in HR, perhaps directly at DNA ends, and that the de-repression of this function can partially overcome the loss of Rad50. Because Mre11-Rad50 is known to encode an endonuclease, we hypothesized that the repair function that is de-repressed when Ku is lost could be provided by an unknown nuclease that resects DNA double-strand break ends in the absence of Ku and Rad50. Exo1 is a good candidate for such a nuclease because over-expression of *EXO1* can suppress the DNA damage sensitivity of *mre11* disruptants in *S. cerevisiae* (30, 41, 58). Thus, if *S. pombe* Exo1 can resect DSB ends independently of the Rad50-Rad32 protein complex, then *rad50 exo1* double mutants should be more sensitive to DNA damage than the

single mutants. To test this, we examined the MMS and the IR sensitivity of *rad50 exo1* double mutants. As shown previously (54), *exo1* single mutants were not significantly IR sensitive (Fig. 3A). However, the *rad50 exo1* double mutant was significantly more IR and MMS sensitive than the single *rad50* mutant (Fig. 3A and B). These results suggest that Rad50 and Exo1 can function independently. Similar results have been reported in *S. cerevisiae*, where *exo1 mre11* double mutants become more MMS-sensitive than in either single mutants (41, 58). Importantly, the MMS sensitivity of the *rad50* mutant was suppressed by deletion of *pku70*$^{+}$ (Fig. 2). However the MMS sensitivity of the *rad50 exo1* double mutant was not suppressed by deletion of *pku70*$^{+}$ (Fig. 3B). The similar results were obtained in the spot tests when *rad32* mutant was used instead of *rad50* mutant (Fig. 3C). These results indicate that the Ku heterodimer may prevent DSB resection by Exo1 in the absence of Rad50-Rad32 protein complex. In agreement with our hypothesis that both Rad50 and Exo1 can act an early step in HR, the rad50 *exo1 double* mutant was as IR sensitive as the *rhp51* single mutant.

Rad50 and Exo1 function independently upstream of Rad51. Treatment

of wild-type *S. pombe* cells with 500 Gy of γ-rays resulted in the formation of Rad51 (Rhp51) foci in almost 100% of cells within 1h post-irradiation (8). If Rad50 and Exo1 function independently and upstream of Rad51, IR-induced Rad51 focus formation should be significantly compromised in *rad50 exo1* double mutants compared to the respective single mutants. Indeed, we find that *rad50-d* cells and *exo1-d* cells showed only a moderate reduction in the focal assembly of Rhp51 following IR (% cells with foci: *rad50-d*, 50% and *exo1-d*, 80%), whereas *rad50 exo1* double mutant cells were strongly impaired in Rhp51 focus formation 1h post-irradiation (% cells with foci: *rad50-d exo1-d*, 8%) (Fig.4). These date are consistent with a model in which Rad50-Rad32 and Exo1 process DNA DSB ends in a redundant manner upstream of Rad51.

Rad50-Rad32 is involved in the production of G-strand overhang in *taz1-d* cells. Our genetic data suggest that the reason that the *S. pombe* Rad50-Rad32 complex is required for DNA damage resistance is most probably because of its role in the processing of DSB ends. The Rad50 complex has also been implicated in the processing of telomere ends (15, 25, 49) and therefore we examined whether these

interactions were reflected in the processing of these specific DNA structures.

Asynchronous wild-type *S. pombe* cells contain only very small amounts of the G-rich overhang at telomeres (2), making it difficult to evaluate the role of Rad50-Rad32 in the processing of telomere ends in wild-type cells (Fig.5B, top panel, lane 2). However, using an in-gel hybridization assay (16), we observed strong signals corresponding to the G-strand overhang in asynchronous *taz1-d* cells (Fig.5A, top panel, lane1). We therefore constructed *taz1 rad50* double mutants and *taz1 rad32* double mutants and examined the extent of the single-stranded overhang at the telomeres. Intriguingly, both *taz1 rad50* double mutants and *taz1 rad32* double mutants lacked the G-strand overhang (Fig.5A, top panel. lanes 2 and 3). These results suggest that the Rad50-Rad32 complex is required either for degradation of the corresponding C-rich strand in *taz1-d* cells or for elongation of the G-rich strand. If Rad32 and Rad50 are required for elongation of the G strand of telomeres, the elongation of telomeres themselves in *taz1 rad32* double mutants would be less efficient than that in *taz1* single mutants. However, the length of telomeres themselves in a *taz1 rad32* double mutant, which was constructed by deletion of $taz1^{+}$ in *rad32-d* cells, was identical to that seen in

the *taz1* single mutant (Fig. 5A, bottom panel. lanes 1 and 3), suggesting that the Rad50-Rad32 complex is not required for G-strand elongation in *taz1-d* cells.

To exclude the possibility that the G-strand overhang in *taz1-d* cells is telomerase dependent, we also created a *taz1 trt1* double mutant, which lacked active telomerase. As shown previously (46, 47), *taz1 trt1* double mutants lost telomeres very rapidly (Fig.5B bottom panel. lane 1), however, the signals corresponding to the G-rich overhang were still detected (Fig.5B, top panel. lane 1). These results indicate that the G-rich overhang in *taz1-d* cells can be generated without telomerase activity, probably through degradation by the Rad50-Rad32 complex. Although degradation of the C-rich strand at the telomere ends in *taz1-d* cells seems to be fully Rad50-Rad32 dependent, in *S. cerevisiae* DNA ends made by HO endonuclease are still processed in *mre11* mutants (29). This difference suggests that telomere ends may be highly protected from degradation even in the absence of Mre11 complex.

Interestingly, as we observed for the sensitivity to DNA damage, inactivation of the Ku heterodimer could overcome the loss of Rad50-Rad32 and restore the G-strand overhang at telomere ends. In a *taz1 rad50 pku70* triple mutant, a significant

amount of G-rich overhang was detected (Fig.5A, top panel, lanes 4 and 5). This again can be interpreted to indicate that an unknown nuclease activity can digest the corresponding C-rich strand to produce the G-rich overhang in the absence of the Rad32-Rad50 complex, and that this nuclease activity is inhibited by the presence of Ku70. However, unlike the situation deduced from the DNA damage sensitivity analysis presented above, this nuclease activity cannot exclusively be attributed to Exo1 activity since we still detect significant levels of G-rich overhang in *taz1 rad50 pku70 exo1* quadruple mutants and *taz1 rad32 pku70 exo1* quadruple mutants (Fig.5A, top panel, lanes 6 and 7). These data suggest that telomere ends are processed by a different mechanism from those of DSB ends.

***rad32* nuclease domain mutants possess G-strand overhang in *taz1-d* cells.**

Our data suggest a model in which the Rad50-Rad32 protein complex is involved in end-processing at DSBs and at telomeres, and further suggest that the Ku hetrodimer negatively influences exonuclease I, which can act on DSBs but not on telomeric ends in the absence of Rad50-Rad32. To test whether the nuclease activity of Rad32 is indeed required for resection of telomeres, we made a *rad32-D25A taz1*double mutant.

Aspartate 25 in the *S. pombe* Rad32 protein corresponds to the catalytically important aspartate residue 8 in the *P. furiosus* Mre11 protein (18). This aspartate coordinates two Mn^{2+} atoms that are located in the active site and are required for the endo/exonuclease activity of *P. furiosus* Mre11 (26). A mutant of the equivalent protein in *S. cerevisiae*, Mre11 D16A, does not possess 5' to 3' exonuclease activity *in vitro* (21). *S. cerevisiae mre11-D16A* mutant strains exhibit MMS sensitivity, but this sensitivity is about 10-fold weaker than that of a null mutant (21). Consistent with the important role of this aspartate, *rad32-D25A* mutants were as MMS and HU sensitive as the *rad32-d* cells (data not shown). These findings are consistent with previously reported data showing that *rad32-D25N* mutants are as γ-ray sensitive as a *rad32* null mutant (65).

Interestingly, *taz1-d rad32-D25A* double-mutants contained a significant amount of the G-strand overhang (Fig.5C, lanes 3 and 4) (two independent clones), indicating that the Rad32 nuclease domain is not required for degradation of the C-rich strand. Our results suggest that, at the telomere ends, the Rad50 complex does not act as nuclease itself but probably recruits an unknown nuclease activity to telomeres. To

ascertain if this nuclease is independent of Exo1, we created *taz1-d exo1-d* double mutants. These *taz1-d exo1-d* double mutants contained a significant G-rich overhang (data not shown), suggesting that the recruited nuclease activity is not exclusively due to Exo1. In *S. cerevisiae*, some of the Mre11 nuclease domain mutants do not form a complex with Rad50 (28). Thus, we tested the interaction between Rad32-D25A and Rad50 by co-immunoprecipitation experiments. We tagged the N-terminus of Rad50 with a TAP-tag (64) and tagged the C-terminus of Rad32 with Myc-tag (1). Cells expressing both tagged proteins were lysed, and Rad50 was affinity precipitated from the soluble lysate with IgG-conjugated magnetic beads (see *MATERIALS AND METHODS*). As expected, Rad32-Myc was co-precipitated with Rad50 (Fig. 5D). Next, we tested the interaction between Rad32-D25A and Rad50. Although the efficiency of protein binding was lower than that of wild-type Rad32, Rad32-D25A retained the ability to interact with Rad50 (Fig. 5D). We also tested the interaction between Rad32-D25A and telomere by chromatin immunoprecipitation (ChIP) assay. As reported previously, telomeric DNA was specifically amplified from Rad32-Myc immunoprecipitate (48). We also found that Rad32-D25A-Myc can bind to telomere

ends (Fig. 5E). These two results strongly suggest that the nuclease mutant Rad32-D25A forms a complex with Rad50 on the telomere DNA. This is consistent with a model where Rad23-D25A can recruit the unknown nuclease to telomere ends.

DISCUSSION

The roles of the Rad50-Rad32 complex and Ku70 complex at DSB ends. *S. pombe* Rad50 and Rad32 are required for efficient HR repair, but their exact roles at DSB ends remain unclear (25, 32, 56, 65, 66). Unlike in *S. cerevisiae*, a method to analyze the rate of degradation of DSB ends has not been developed for *S. pombe*. This makes it difficult to study the roles of the Rad32-Rad50 complex at DSB ends. We have demonstrated that *rad50 exo1* double mutants are more IR sensitive than the respective single mutants and are as sensitive as cells lacking Rad51 (Rhp51) (Fig. 3A). Consistent with this observation, a *rad50 exo1* double mutant was strongly impaired in the formation of Rhp51 foci after irradiation (Fig. 4). These results are fully consistent with a model in which the Rad50-Rad32 complex and Exo1 can independently and redundantly act on DNA DSB ends to generate the substrates for Rhp51 filament formation (Fig. 6 A).

We also found that both the MMS and IR sensitivities of *rad50-d* cells were suppressed by concomitant deletion of *pku70*$^{+}$, which encodes the Ku70 protein required for an early step in NHEJ (Fig. 1). However, the MMS sensitivity of the *rad50 exo1*

double mutants was not suppressed by deletion of *pku70*$^{+}$ (Fig. 3B). In *S. cerevisiae*, it has been suggested that Ku competes with 5' to 3' exonucleases at DNA ends (29). However, the nuclease competing with Yku70 has not been identified. Our results strongly suggest that the nuclease competing with Ku70 at DSB ends is ExoI (Fig. 6 A). In contrast to the competition between Ku and ExoI, the Rad50 complex can process DSB ends in the presence of Ku heterodimer. *pku70-d* cells are not IR sensitive (32), suggesting that Ku70 does not recruit the Rad50 complex to the DNA ends. Although the biological significance of the ExoI pathway for HR repair is not clear, Ku might be removed in a controlled manner and protect DSBs from nonspecific degradation in the absence of certain activities.

Is a DNA double-strand break produced following exposure to UV, MMS and HU? The sensitivities of *rad50-d* cells to IR, UV, MMS and HU were all suppressed by concomitant deletion of *pku70*$^{+}$ (Fig. 1A-D). This suggests that, in the absence of *rad50*$^{+}$, γ-rays, UV light, MMS and HU cause the generation of similar DNA structures, probably DSBs, that may be bound by the Ku70-Ku80 heterodimer. However, the suppression of the UV sensitivity is potentially confusing because UV light produces

primarily CPDs or 6-4 photoproducts, not DSBs. Recombination is much more important for UV survival in *S. pombe* than in budding yeast, as shown by the fact that *rad22*, *rhp51* and *rhp54* mutants are all significantly UV-sensitive (36). To initiate homologous recombination, DNA double-strand breaks should be generated. Interestingly, in *S. pombe*, CPDs and 6-4 photoproducts are not only repaired by the NER pathway but also by the UVDE pathway, which facilitates homologous recombination (36). Furthermore, unrepaired UV-induced lesions are thought to become substrates for HR-based post-replication repair processes when encountered by a replication fork. Thus, DNA double-strand breaks could be produced as a secondary lesion during the recombinogenic recovery from UV damage. A similar mechanism probably underlies the HU and MMS sensitivity of *rad50-d* cells. Both HU and MMS can stall the replication fork and such stalled forks can result in DSBs , as shown in *E. coli* (27, 37). It is now becoming clear that in many eukaryotes, including *S. pombe*, DNA double-strand breaks can be produced by replication arrest and that HR is required for their repair (44, 45). In *S. pombe*, a Holliday junction formed at a stalled or collapsed replication fork is thought to either be reversed by Rqh1 helicase in a

nonrecombinogenic pathway or resolved by a Mus81-Eme1-dependent endonuclease (potentially via a recombinogenic pathway) (5, 17). In the latter case, DSBs are suggested to be produced to initiate homologous recombination.

Given that IR, UV, MMS and HU could all cause double-strand breaks in *S. pombe*, suppression of the sensitivity of *rad50-d* cells to all these agents by the concomitant deletion of *pku70*$^{+}$ could be explained by a model in which the Ku heterodimer has to be removed from the break site in the absence of Rad50 to allow end processing by alternative nucleases (Fig. 6 A).

Roles of Rad32-Rad50 complex and Ku70 at the telomere ends in *taz1-d* cells. Both the Rad50-Rad32 protein complex and the Ku heterodimer are involved not only in the processing of DSBs but also in telomere maintenance (25, 66). However, it is unknown how these proteins act to regulate telomere length. Asynchronous *taz1*-d cells contain extensive G-rich single-stranded 3' overhangs at telomere ends (Fig.5A, top panel, lane1), making it possible to study the roles of Rad50, Ku70 and Exo1 at these telomeres. As shown in Fig. 5B (top panel, lane1), the generation of the G-rich overhang in *taz1-d* cells occurs in the absence of telomerase

activity, suggesting that the G-rich overhang is generated by degradation of the C-rich strand. Our results suggest that this nuclease step is dependent on the Rad32-Rad50 complex without utilizing its nuclease activity, because the G-rich overhang in *taz1-d* cells disappeared upon deletion of either *rad50*$^{+}$or *rad32*$^{+}$ (Fig. 5A, top panel, lanes 2 and 3) but not upon mutation of the nuclease domain of Rad32 (Fig. 5C, top panel, lanes 3 and 4). To explain the physical requirement for Rad32, we propose that (in *taz1* disruptants) the Rad50-Rad32 complex recruits an unknown nuclease, which contains 5' to 3' exonuclease activity, to the telomere (Fig. 6 B). We do not know which nuclease is recruited. However, we can exclude the major activity being due to Exo1, because *taz1-d exo1-d* double mutants contained significant G-rich overhangs (data not shown). Although the biological significance of the Rad50-Rad32-dependent generation of G-rich overhang in *taz1-d* cells is not clear, Taz1 may be detached from telomeric DNA during telomere elongation. Therefore our results may be reflecting the function of these proteins during telomere elongation.

Recently, it has been suggested that ExoI is required for both ssDNA generation at telomeres and the subsequent cell cycle arrest of *yku70* mutants in *S.*

cerevisiae (34). Our results in *S. pombe* are not consistent with this: we found that no detectable role for ExoI at telomere ends. It is possible that there are significant differences between *S. pombe* and *S. cerevisiae*, or that the different assays used affect competing activities in distinct ways.

The roles of Rad32-Rad50 at DSB ends. The importance of nuclease activity in Rad32 for the processing of DBS ends remains clear. Although Mre11 has a 3' to 5' exonuclease and endonuclease activity *in vitro* (51, 57), *in vivo* observations suggest that Mre11 is required for the oppositely oriented (5' to 3') exonuclease activity (29). There are two possible models to explain this discrepancy. (1) A long 3' ssDNA is generated by the endonuclease activity of Rad32 combined with unidentified helicase components. (2) An unidentified 5' to 3' exonuclease is recruited to DSB ends by a Rad32 (Mre11) complex. At this point it is difficult to distinguish these two possibilities, and further studies are required to resolve this discrepancy. It has been reported that the *in vivo* 5' to 3' resection of DNA ends is strongly dependent upon the successful formation of the Mre11 protein complex, perhaps along with other, as yet unidentified components (28). We found that Rad32 nuclease domain mutants were

significantly MMS sensitive (data not shown). However, we can not conclude that the nuclease activity in Rad32 is required for the processing of DBS ends, because the interaction between Rad32-D25A and Rad50 were less efficient than that the interaction between Rad32 and Rad50 (Fig. 5D). The reduced stability of Rad32-D25A-Rad50 complex may impair the 5' to 3' resection ability by affecting the unknown function of the Rad32-Rad50 complex, perhaps binding to unidentified proteins. As suggested the roles of Rad32-Rad50 complex at telomere ends in *taz1-d* cells, the main roles of the Rad50 complex might be the recruitment of unidentified nuclease or other factors to DSB ends. These factors are also suggested to exist in *S. cerevisiae* (28).

Conclusion. Our data suggest that the Rad50 complex is required for the processing of DSB ends and telomere ends in the presence of Ku heterodimer. However, Ku heterodimer inhibits processing of DSB ends and telomere ends by alternative nucleases in the absence of the Rad50-Rad32 protein complex. While we have identified Exo1 as the alternative nuclease targeting DNA break sites, the identity of the nuclease acting on the telomere ends remains elusive. The nuclease function of the Rad50-Rad32 protein complex seems to not be important for degradation of the

C-rich strand at telomeres. Moreover, our data allow the speculation that cells regulate the resection of DNA ends in the absence of Rad50 complex through controlled binding of the Ku heterodimer. A similar regulation might underlie the cell-cycle-specific appearance of the G-rich overhang at telomeres.

ACKNOWLEDGEMENTS

We thank Kohta Takahashi, Shigeaki Saitoh and Mitsuhiro Yanagida for ChIP assay protocol, and Hiroyuki Araki for helping with UV-irradiation experiments, and Takeshi Saito, Shinji Yasuhira and Hiroshi Utsumi for helping with γ-ray irradiation, and Masayuki Yamamoto for providing strains, and John R. Pringle for providing plasmid. This work was supported by Grants-in-Aid for Scientific Research on Priority Areas from the Ministry of Education, Science, Sports and Culture of Japan to A. M., K.O., and M. U. Part of this work was performed under the Basic Research 21 for Breakthroughs in Info-Communications project supported by the Ministry of Public Management, Home Affairs, Posts and Telecommunications and the Support Center for Advanced Telecommunications Technology Research Foundation to M.U.

REFERENCES

1. **Bahler, J., J. Q. Wu, M. S. Longtine, N. G. Shah, A. McKenzie, 3rd, A. B. Steever, A. Wach, P. Philippsen, and J. R. Pringle.** 1998. Heterologous modules for efficient and versatile PCR-based gene targeting in *Schizosaccharomyces pombe*. Yeast **14:**943-51.

2. **Baumann, P., and T. R. Cech.** 2001. Pot1, the putative telomere end-binding protein in fission yeast and. Science **292:**1171-5.

3. **Baumann, P., and T. R. Cech.** 2000. Protection of telomeres by the Ku protein in fission yeast. Mol. Biol. Cell. **11:**3265-75.

4. **Blackburn, E. H.** 2001. Switching and signaling at the telomere. Cell **106:**661-73.

5. **Boddy, M. N., A. Lopez-Girona, P. Shanahan, H. Interthal, W. D. Heyer, and P. Russell.** 2000. Damage tolerance protein Mus81 associates with the FHA1 domain of checkpoint kinase Cds1. Mol. Cell. Biol. **20:**8758-66.

6. **Boulton, S. J., and S. P. Jackson.** 1998. Components of the Ku-dependent non-homologous end-joining pathway are involved in telomeric length

maintenance and telomeric silencing. EMBO J. **17:**1819-28.

7. **Bressan, D. A., B. K. Baxter, and J. H. Petrini.** 1999. The Mre11-Rad50-Xrs2 protein complex facilitates homologous recombination-based double-strand break repair in *Saccharomyces cerevisiae*. Mol. Cell. Biol. **19:**7681-7.

8. **Caspari, T., J. M. Murray, and A. M. Carr.** 2002. Cdc2-cyclin B kinase activity links Crb2 and Rqh1-topoisomerase III. Genes Dev. **16:**1195-208.

9. **Cohn, M., and E. H. Blackburn.** 1995. Telomerase in yeast. Science **269:**396-400.

10. **Conrad, M. N., J. H. Wright, A. J. Wolf, and V. A. Zakian.** 1990. RAP1 protein interacts with yeast telomeres in vivo: overproduction alters. Cell **63:**739-50.

11. **Cooper, J. P., E. R. Nimmo, R. C. Allshire, and T. R. Cech.** 1997. Regulation of telomere length and function by a Myb-domain protein in fission yeast. Nature **385:**744-7.

12. **Critchlow, S. E., and S. P. Jackson.** 1998. DNA end-joining: from yeast to man. Trends. Biochem. Sci. **23:**394-8.

13. **Cromie, G. A., J. C. Connelly, and D. R. Leach.** 2001. Recombination at double-strand breaks and DNA ends: conserved mechanisms. Mol. Cell. **8:**1163-74.

14. **D'Amours, D., and S. P. Jackson.** 2002. The Mre11 complex: at the crossroads of dna repair and checkpoint signalling. Nat. Rev. Mol. Cell. Biol. **3:**317-27.

15. **Diede, S. J., and D. E. Gottschling.** 2001. Exonuclease activity is required for sequence addition and Cdc13p loading at a de novo telomere. Curr. Biol. **11:**1336-40.

16. **Dionne, I., and R. J. Wellinger.** 1996. Cell cycle-regulated generation of single-stranded G-rich DNA in the. Proc. Natl. Acad. Sci. U S A **93:**13902-7.

17. **Doe, C. L., J. S. Ahn, J. Dixon, and M. C. Whitby.** 2002. Mus81-Eme1 and Rqh1 involvement in processing stalled and collapsed replication forks. J. Biol. Chem. **277:**32753-9.

18. **Farah, J. A., E. Hartsuiker, K. Mizuno, K. Ohta, and G. R. Smith.** 2002. A 160-bp palindrome is a Rad50•Rad32-dependent mitotic recombination hotspot in *Schizosaccharomyces pombe*. Genetics **161:**461-8.

19. **Featherstone, C., and S. P. Jackson.** 1999. Ku, a DNA repair protein with multiple cellular functions? Mutat. Res. **434:**3-15.

20. **Ferreira, M. G., and J. P. Cooper.** 2001. The fission yeast Taz1 protein protects chromosomes from Ku-dependent end-to-end fusions. Mol. Cell. **7:**55-63.

21. **Furuse, M., Y. Nagase, H. Tsubouchi, K. Murakami-Murofushi, T. Shibata, and K. Ohta.** 1998. Distinct roles of two separable in vitro activities of yeast Mre11 in mitotic and meiotic recombination. EMBO J. **17:**6412-25.

22. **Gu, Y., K. J. Seidl, G. A. Rathbun, C. Zhu, J. P. Manis, N. van der Stoep, L. Davidson, H. L. Cheng, J. M. Sekiguchi, K. Frank, P. Stanhope-Baker, M. S. Schlissel, D. B. Roth, and F. W. Alt.** 1997. Growth retardation and leaky SCID phenotype of Ku70-deficient mice. Immunity **7:**653-65.

23. **Haber, J. E.** 1998. The many interfaces of Mre11. Cell **95:**583-6.

24. **Haber, J. E.** 1999. Sir-Ku-itous routes to make ends meet. Cell **97:**829-32.

25. **Hartsuiker, E., E. Vaessen, A. M. Carr, and J. Kohli.** 2001. Fission yeast Rad50 stimulates sister chromatid recombination and links cohesion with repair.

EMBO J. **20:**6660-71.

26. **Hopfner, K. P., A. Karcher, L. Craig, T. T. Woo, J. P. Carney, and J. A. Tainer.** 2001. Structural biochemistry and interaction architecture of the DNA double-strand break repair Mre11 nuclease and Rad50-ATPase. Cell **105:**473-85.

27. **Kowalczykowski, S. C.** 2000. Initiation of genetic recombination and recombination-dependent replication. Trends. Biochem. Sci. **25:**156-65.

28. **Lee, S. E., D. A. Bressan, J. H. Petrini, and J. E. Haber.** 2002. Complementation between N-terminal *Saccharomyces cerevisiae mre11* alleles in DNA repair and telomere length maintenance. DNA Repair (Amst) **1:**27-40.

29. **Lee, S. E., J. K. Moore, A. Holmes, K. Umezu, R. D. Kolodner, and J. E. Haber.** 1998. Saccharomyces Ku70, mre11/rad50 and RPA proteins regulate adaptation to G2/M arrest after DNA damage. Cell **94:**399-409.

30. **Lewis, L. K., G. Karthikeyan, J. W. Westmoreland, and M. A. Resnick.** 2002. Differential suppression of DNA repair deficiencies of Yeast *rad50*, *mre11* and *xrs2* mutants by EXO1 and TLC1 (the RNA component of

telomerase). Genetics **160:**49-62.

31. **Lustig, A. J., S. Kurtz, and D. Shore.** 1990. Involvement of the silencer and UAS binding protein RAP1 in regulation of telomere length. Science **250:**549-53.

32. **Manolis, K. G., E. R. Nimmo, E. Hartsuiker, A. M. Carr, P. A. Jeggo, and R. C. Allshire.** 2001. Novel functional requirements for non-homologous DNA end joining in *Schizosaccharomyces pombe*. EMBO J. **20:**210-21.

33. **Marchetti, M. A., S. Kumar, E. Hartsuiker, M. Maftahi, A. M. Carr, G. A. Freyer, W. C. Burhans, and J. A. Huberman.** 2002. A single unbranched S-phase DNA damage and replication fork blockage checkpoint pathway. Proc. Natl. Acad. Sci. U S A **99:**7472-7.

34. **Maringele, L., and D. Lydall.** 2002. EXO1-dependent single-stranded DNA at telomeres activates subsets of DNA damage and spindle checkpoint pathways in budding yeast *yku70*Delta mutants. Genes Dev. **16:**1919-33.

35. **Martin, S. G., T. Laroche, N. Suka, M. Grunstein, and S. M. Gasser.** 1999. Relocalization of telomeric Ku and SIR proteins in response to DNA strand

breaks in yeast. Cell **97:**621-33.

36. **McCready, S. J., F. Osman, and A. Yasui.** 2000. Repair of UV damage in the fission yeast *Schizosaccharomyces pombe*. Mutat. Res. **451:**197-210.

37. **Michel, B., S. D. Ehrlich, and M. Uzest.** 1997. DNA double-strand breaks caused by replication arrest. EMBO J. **16:**430-8.

38. **Milne, G. T., S. Jin, K. B. Shannon, and D. T. Weaver.** 1996. Mutations in two Ku homologs define a DNA end-joining repair pathway in *Saccharomyces cerevisiae*. Mol. Cell. Biol. **16:**4189-98.

39. **Miyoshi, T., M. Sadaie, J. Kanoh, and F. Ishikawa.** 2003. Telomeric DNA ends are essential for the localization of ku at telomeres in fission yeast. J. Biol. Chem. **278:**1924-31.

40. **Moreau, S., J. R. Ferguson, and L. S. Symington.** 1999. The nuclease activity of Mre11 is required for meiosis but not for mating type switching, end joining, or telomere maintenance. Mol. Cell. Biol. **19:**556-66.

41. **Moreau, S., E. A. Morgan, and L. S. Symington.** 2001. Overlapping functions of the *Saccharomyces cerevisiae* Mre11, Exo1 and Rad27 nucleases in DNA

metabolism. Genetics **159:**1423-33.

42. **Moreno, S., A. Klar, and P. Nurse.** 1991. Molecular genetic analysis of fission yeast *Schizosaccharomyces pombe*. Methods Enzymol. **194:**795-823.

43. **Muris, D. F., K. Vreeken, A. M. Carr, B. C. Broughton, A. R. Lehmann, P. H. Lohman, and A. Pastink.** 1993. Cloning the RAD51 homologue of *Schizosaccharomyces pombe*. Nucleic Acids Res. **21:**4586-91.

44. **Muris, D. F., K. Vreeken, A. M. Carr, J. M. Murray, C. Smit, P. H. Lohman, and A. Pastink.** 1996. Isolation of the *Schizosaccharomyces pombe* RAD54 homologue, *rhp54*$^{+}$, a gene involved in the repair of radiation damage and replication fidelity. J. Cell. Sci. **109 (Pt 1):**73-81.

45. **Murray, J. M., H. D. Lindsay, C. A. Munday, and A. M. Carr.** 1997. Role of *Schizosaccharomyces pombe* RecQ homolog, recombination, and checkpoint genes in UV damage tolerance. Mol. Cell. Biol. **17:**6868-75.

46. **Nakamura, T. M., J. P. Cooper, and T. R. Cech.** 1998. Two modes of survival of fission yeast without telomerase. Science **282:**493-6.

47. **Nakamura, T. M., G. B. Morin, K. B. Chapman, S. L. Weinrich, W. H.**

Andrews, J. Lingner, C. B. Harley, and T. R. Cech. 1997. Telomerase catalytic subunit homologs from fission yeast and human. Science **277:**955-9.

48. **Nakamura, T. M., B. A. Moser, and P. Russell.** 2002. Telomere binding of checkpoint sensor and DNA repair proteins contributes to maintenance of functional fission yeast telomeres. Genetics **161:**1437-52.

49. **Nugent, C. I., G. Bosco, L. O. Ross, S. K. Evans, A. P. Salinger, J. K. Moore, J. E. Haber, and V. Lundblad.** 1998. Telomere maintenance is dependent on activities required for end repair of double-strand breaks. Curr. Biol. **8:**657-60.

50. **Paques, F., and J. E. Haber.** 1999. Multiple pathways of recombination induced by double-strand breaks in *Saccharomyces cerevisiae*. Microbiol. Mol. Biol. Rev. **63:**349-404.

51. **Paull, T. T., and M. Gellert.** 1998. The 3' to 5' exonuclease activity of Mre 11 facilitates repair of DNA double-strand breaks. Mol. Cell. **1:**969-79.

52. **Siede, W., A. A. Friedl, I. Dianova, F. Eckardt-Schupp, and E. C. Friedberg.** 1996. The *Saccharomyces cerevisiae* Ku autoantigen homologue affects radiosensitivity only in the absence of homologous recombination. Genetics

142:91-102.

53. **Sugawara, N., and J. E. Haber.** 1992. Characterization of double-strand break-induced recombination: homology requirements and single-stranded DNA formation. Mol. Cell. Biol. **12:**563-75.

54. **Szankasi, P., and G. R. Smith.** 1995. A role for exonuclease I from *S. pombe* in mutation avoidance and mismatch correction. Science **267:**1166-9.

55. **Takahashi, K., S. Saitoh, and M. Yanagida.** 2000. Application of the chromatin immunoprecipitation method to identify in vivo protein-DNA associations in fission yeast. Sci. STKE **2000:**PL1.

56. **Tavassoli, M., M. Shayeghi, A. Nasim, and F. Z. Watts.** 1995. Cloning and characterisation of the *Schizosaccharomyces pombe rad32* gene: a gene required for repair of double strand breaks and recombination. Nucleic Acids Res. **23:**383-8.

57. **Trujillo, K. M., S. S. Yuan, E. Y. Lee, and P. Sung.** 1998. Nuclease activities in a complex of human recombination and DNA repair factors Rad50, Mre11, and p95. J. Biol. Chem. **273:**21447-50.

58. **Tsubouchi, H., and H. Ogawa.** 2000. Exo1 roles for repair of DNA double-strand breaks and meiotic crossing over in *Saccharomyces cerevisiae*. Mol. Biol. Cell. **11:**2221-33.

59. **Tsukamoto, Y., J. Kato, and H. Ikeda.** 1996. Effects of mutations of RAD50, RAD51, RAD52, and related genes on illegitimate recombination in *Saccharomyces cerevisiae*. Genetics **142:**383-91.

60. **Tsukamoto, Y., J. Kato, and H. Ikeda.** 1996. Hdf1, a yeast Ku-protein homologue, is involved in illegitimate recombination, but not in homologous recombination. Nucleic Acids Res. **24:**2067-72.

61. **Usui, T., T. Ohta, H. Oshiumi, J. Tomizawa, H. Ogawa, and T. Ogawa.** 1998. Complex formation and functional versatility of Mre11 of budding yeast in recombination. Cell **95:**705-16.

62. **van Steensel, B., and T. de Lange.** 1997. Control of telomere length by the human telomeric protein TRF1. Nature **385:**740-3.

63. **Vogel, H., D. S. Lim, G. Karsenty, M. Finegold, and P. Hasty.** 1999. Deletion of Ku86 causes early onset of senescence in mice. Proc. Natl. Acad. Sci. U S A

96:10770-5.

64. **Werler, P. J., E. Hartsuiker, and A. M. Carr.** 2003. A simple Cre-loxP method for chromosomal N-terminal tagging of essential and non-essential *Schizosaccharomyces pombe* genes. Gene **304:**133-41.

65. **Wilson, S., M. Tavassoli, and F. Z. Watts.** 1998. *Schizosaccharomyces pombe rad32* protein: a phosphoprotein with an essential phosphoesterase motif required for repair of DNA double strand breaks. Nucleic Acids Res. **26:**5261-9.

66. **Wilson, S., N. Warr, D. L. Taylor, and F. Z. Watts.** 1999. The role of *Schizosaccharomyces pombe* Rad32, the Mre11 homologue, and other DNA damage response proteins in non-homologous end joining and telomere length maintenance. Nucleic Acids Res. **27:**2655-61.

FIGURE LEGENDS

Fig.1 **DNA damage sensitivity of *rad50-d* cells is suppressed by deletion of *pku70*$^{+}$.** (**A-D**). The sensitivities to γ-rays, HU, MMS and UV light of *rad50-d* cells□ and *rad50 pku70* double mutants. The survival (%; y-axis) of wild-type cells, JY741 (closed circles), *rad50-d,* KT002 (closed triangles), and *rad50 pku70* double mutants, KT152 (open triangles) are plotted against the dose of gamma-rays (A: Gy; x-axis), or UV light (B: J/m^2; x-axis), or plotted against time in 20 mM HU (D: hours; x-axis), or 0.02% MMS (C: hours; x-axis). Standard deviations are shown by error bars.

Fig. 2 **Suppression of DNA damage sensitivity occurs upstream of Rad51.** Cell survival frequencies on 0.002% MMS-containing plates versus control plates for wild-type cells (JY741), *rad50-d* (KT002), *rhp51-d* (KT00c), *rhp51-d pku70-d* (KT10c5), *pku80-d* (KT090), *rad50-d pku80-d* (KT192), *lig4-d* (KT1a0) and *rad50-d lig4-d* cells (KT1a2). Standard deviations are shown by error bars (for two to four independent experiments).

Fig.3 ***rad50 exo1*** **double mutants become more DNA-damage sensitive than each single mutants.** (**A**) The sensitivities to γ-rays of wild-type cells, *rad50-d*, *exo1-d*, *rad50-d exo1-d* and *rhp51-d* cells. The survival (%; y-axis) of wild-type cells (700), *rad50-d* (701), *exo1-d* (702), *rad50-d exo1-d* (703) and *rhp51-d* cells (704) is plotted against the gamma-ray dose (Gy; x-axis). (**B**) Cell survival frequencies on 0.002% MMS-containing plates versus control plates for wild-type cells (JY741), *exo1-d* (KT00g), *rad50-d* (KT002), *rad50-d exo1-d* (KT02g), *pku70-d rad50-d exo1-d* (KT12g5) □□□□□□ Standard deviations are shown by error bars (for two to four independent experiments). (**C**) The MMS sensitivity of wild-type cells (119), *rad32-d* (324), *rad32-d pku70-d* (315), *rad32-d exo1-d* (403), *pku70-d rad32-d exo1-d* (407), *pku70-d* (319), *exo1-d* (302), and *exo1-d pku70-d* (394) cells was assayed by the spot test. The cells were grown in YEA ($0.5x10^7$ cells/ml), serially diluted (1:10) with sterilized water, and spotted 4μl of each dilution were spotted onto the MMS plates.

Fig. 4 **Exo1 and rad50 function independently upstream of Rad51.** (**A**) Indirect immunofluorescence microscopy of wild-type cells (700), *rad50-d* (701), *exo1-d* (702),

and *rad50-d exo1-d* □□□ls (703) at 1h after irradiation with 500 Gy of ionizing radiation (8). A cross-reacting human anti-Rad51 antibody was used to detect Rhp51. (**B**) Mean percentage of various mutant cells showing Rhp51 foci at 1h post-irradiation.

Fig.5 **The roles of Rad50 and Ku70 at telomere ends in *taz1-d* cells.** (**A-C**) The single-stranded overhangs were detected by in-gel hybridization. (**A**) Lane1, *taz1-d* (KT110). Lane2, *rad50-d taz1-d* (KT021). Lane 3, *rad32-d taz1-d* (KT116). Lane 4, *pku70-d rad50-d taz1-d* (KT215). Lane 5, *pku70-d rad32-d taz1-d* (KT1165). Lane 6, *pku70-d rad50-d exo1-d taz1-d* (KT121g5). Lane 7, *pku70-d rad32-d exo1-d taz1-d* (KT016g5). Lane 8, dsDNA control. Lane 9, ssDNA control. (**B**) Lane 1, *taz1-d trt1-d* (KT117). Lane 2, wild-type cells (JY741). Lane 3, dsDNA control. Lane 4, ssDNA control. (**C**) Lane1, *taz1-d* (KT110). Lane2, *rad32-d taz1-d*. (KT116). Lane 3, *rad32-D25A taz1-d* (KT0106M1). Lane 4, *rad32-D25A taz1-d* (KT0106M2). Lane 5, dsDNA control. Lane 6, ssDNA control. Genomic DNAs were digested with *Eco*RI and separated by electrophoresis on a 0.5% agarose gel. Then the gel was dried and hybridized with ^{32}P-labeled C-rich (top panel) or G-rich (middle panel) probe. To

detect double-stranded telomere DNAs, the gel was treated with denaturant and re-probed with C-rich probe (bottom panel). As a control, a linearized telomeric DNA-containing plasmid was used for double-stranded telomere detection. For the single-strand control, heat denatured the same linearized plasmid was used (see *MATERIALS AND METHODS*). Telomere DNA is indicated by arrows. (**D**) Rad32-D25A binds to Rad50 in immunoprecipitation assay. TAP-tagged Rad50 were precipitated with IgG-conjugated magnetic beads from a lysate of *TAP-rad50 rad32-Myc* (KTt2T6M) cells (lane 3 and 8) and a lysate of *TAP-rad50 rad32-D25A-Myc* (KTt2T6MM1) cells (lane 4 and 9), respectively. The immunoprecipitates (IP with IgG) were examined by Western blot (Western) with anti-Myc antibody (anti-Myc). The protein A tag is detected with anti-Protein A antibody (anti-Protein A). *TAP-rad50* cells (435); lane 5 and 10, *rad32-Myc* (KTt6M) cells; lane 1 and 6, and *rad32-D25A-Myc* (KTt6MM1) cells; lane 2 and 7, were used as controls. The same levels of proteins were detected in the whole-cell extract (WCE). (**E**) Rad32-D25A is bound to telomere DNA in ChIP assay. Untagged wild-type control cells (JY741), *rad32-Myc* (KTt6M) cells, and *rad32-D25AMyc* (KTt6MM1)

cells were used. PCRs were performed on whole-cell extract (WCE) and on chromatin immunoprecipitates (IP with anti-Myc) using primers to amplify a telomere DNA (telomere) and primers to amplify DNA from the *ade6*$^{+}$ gene (*ade6*). M represents DNA maker.

Fig. 6 **Models.** (**A**) **Hypothetical model for DSB processing by Rad50 complex and Exo1**. DSB ends are processed mainly by the Rad50-Rad32 complex. In the absence of Rad50-Rad32 complex, DNA ends can be processed by Exo1, but Ku heterodimer has to be removed from the break site to allow end processing. The Cdc13 function may act through the Exo1 pathway, in parallel to Rad50 (8). (**B**) **Hypothetical model for degradation of C-rich strand at telomere ends in *taz1-d* cells**. Telomere ends in *taz1-d* cells are processed mainly by the Rad50-Rad32 complex. Because the nuclease domain is not required for this process, we assume that the Rad50 complex recruits an unknown nuclease. In the absence of Rad50 complex, DNA ends can be processed by unknown nucleases, but Ku heterodimer has to be removed from the break site to allow end processing.

TABLE 1. *S. pombe* strains used in this study

Strain	Genotype	Source
119	*h⁻ smt-0 leu1-32 ura4-D18 his3-D1 arg3-D1*	Lab stock
142	*h⁺ leu1-32 ura4-D18 ade6-M210 rad32::ura4⁺*	This work
302	*smt-0 leu1-32 ura4-D18 his3-D1 arg3-D1 exo1-1::ura4⁺*	This work
315	*smt-0 leu1-32 ura4-D18 his3-D1 arg3-D1 pku70::LEU2 rad32::ura4⁺*	This work
319	*smt-0 leu1-32 ura4-D18 his3-D1 arg3-D1 pku70::LEU2*	This work
324	*smt-0 leu1-32 ura4-D18 his3-D1 arg3-D1 rad32::ura4⁺*	This work
394	*smt-0 leu1-32 ura4-D18 his3-D1 arg3-D1 pku70::LEU2 exo1-1::ura4⁺*	This work
403	*smt-0 leu1-32 ura4-D18 his3-D1 arg3-D1 exo1-1::ura4⁺ rad32::ura4⁺*	This work
407	*smt-0 leu1-32 ura4-D18 his3-D1 arg3-D1 exo1-1::ura4⁺ rad32::ura4⁺ pku70::LEU2*	This work
435	*h⁺ TAP-rad50 ura4-D18 ade6-704 leu1-32*	Lab stock

700	*h*$^{+}$ *leu1-32 ura4-D18*	Lab stock
701	*smt-0 ura4-D18 rad50::kanMX6*	Lab stock
702	*h*$^{+}$ *leu1-32 ura4-D18 exo1::ura4*$^{+}$	Lab stock
703	*h*$^{+}$ *ura4-D18 exo1::ura4*$^{+}$ *rad50::kanMX6*	This work
704	*h*$^{+}$ *leu1-32 ura4-D18 ade6-M216 rhp51::ura4*$^{+}$	Lab stock
KT00c	*h*$^{-}$ *leu1-32 ura4-D18 ade6-M216 rhp51::ura4*$^{+}$	This work
KT00g	*h*$^{-}$ *leu1-32 ura4-D18 ade6-M216 exo1::ura4*$^{+}$	This work
KT001	*h*$^{-}$ *leu1-32 ura4-D18 ade6-M216 taz1::ura4*$^{+}$	This work
KT002	*h*$^{-}$ *leu1-32 ura4-D18 ade6-M216 rad50::ura4*$^{+}$	This work
KT007	*h*$^{-}$ *leu1-32 ura4-D18 ade6-M216 trt1::ura4*$^{+}$	This work
KT0106M1	*h*$^{-}$ *leu1-32 rad32D25A taz1::LEU2*	This work
KT0106M2	*h*$^{-}$ *leu1-32 rad32D25A taz1::LEU2*	This work
KT016g5	*h*$^{-}$ *leu1-32 ura4-D18 ade6-M216 taz1::LEU2 rad32::ura4*$^{+}$ *exo1::ura4*$^{+}$ *pku70::LEU2::ade6*$^{+}$	This work

KT02g	*h*$^{+}$ *leu1-32 ura4-D18 ade6-M216 exo1::ura4*$^{+}$ *rad50::LEU2*	This work
KT021	*h*$^{-}$ *leu1-32 ura4-D18 ade6-M216 rad50::LEU2 taz1::ura4*$^{+}$	This work
KT0215	*h*$^{-}$ *leu1-32 ura4-D18 ade6-M210 rad50::LEU2 taz1::ura4*$^{+}$ *pku70::LEU2::ade6*$^{+}$	This work
KT090	*h*$^{-}$ *leu1-32 ura4-D18 ade6-M216 pku80::LEU2*	This work
KT1a0	*h*$^{+}$ *leu1-32 ura4-D18 ade6-M210 lig4::LEU2*	This work
KT1a2	*h*$^{+}$ *leu1-32 ura4-D18 ade6-M210 lig4::LEU2 rad50::ura4*$^{+}$	This work
KT10c5	*h*$^{+}$ *leu1-32 ura4-D18 ade6 rhp51::ura4*$^{+}$ *pku70::LEU2::ade6*$^{+}$	This work
KT110	*h*$^{+}$ *leu1-32 ura4-D18 ade6-M210 taz1::LEU2*	This work
KT116	*h*$^{+}$ *leu1-32 ura4-D18 ade6-M210 taz1::LEU2 rad32::ura4*$^{+}$	This work

KT1165	*h*$^{+}$ *leu1-32 ura4-D18 ade6-M210 taz1::LEU2 rad32::ura4*$^{+}$ *pku70::LEU2::ade6*$^{+}$	This work
KT117	*h*$^{+}$ *leu1-32 ura4-D18 ade6-M210 taz1::LEU2 trt1::ura4*$^{+}$	This work
KT12g5	*h*$^{-}$ *leu1-32 ura4-D18 ade6- exo1::ura4*$^{+}$ *rad50::LEU2 pku70:: LEU2::ade6*$^{+}$	This work
KT120	*h*$^{-}$ *leu1-32 ura4-D18 ade6-M216 rad50::LEU2*	This work
KT121g5	*h*$^{+}$ *leu1-32 ura4-D18 ade6-M210 rad50::LEU2 taz1::ura4*$^{+}$ *exo1::ura4*$^{+}$ *pku70::LEU2::ade6*$^{+}$	This work
KT192	*h*$^{+}$ *leu1-32 ura4-D18 ade6-M216 pku80::LEU2 rad50::ura4*$^{+}$	This work
KT152	*h*$^{+}$ *leu1-32 ura4-D18 ade6-M216 rad50::ura4*$^{+}$ *pku70::LEU2*	This work
KT156	*h*$^{+}$ *leu1-32 ura4-D18 ade6-M216 rad32::ura4*$^{+}$ *pku70::LEU2*	This work

KTt2T6M	*h*$^{+}$ *leu1-32 ura4-D18 ade6-704 TAP-rad50 rad32-myc:kanMX*	This work
KTt2T6MM1	*h*$^{+}$ *leu1-32 ura4-D18 ade6-704 TAP-rad50 rad32D25A-myc:kanMX*	This work
KTt6M	*h*$^{-}$ *leu1-32 ura4-D18 ade6-M210 rad32-myc:kanMX*	This work
KTt6MM1	*h*$^{-}$ *leu1-32 rad32D25A-myc:kanMX*	This work
JY741	*h*$^{-}$ *leu1-32 ura4-D18 ade6-M216*	M. Yamamoto
pku70L	*h*$^{-}$ *leu1-32 ura4-D18 ade6-M216 pku70::LEU2*	This work
pku70A	*h*$^{-}$ *leu1-32 ura4-D18 ade6-M216 pku70:: LEU2::ade6*$^{+}$	This work

Fig.1

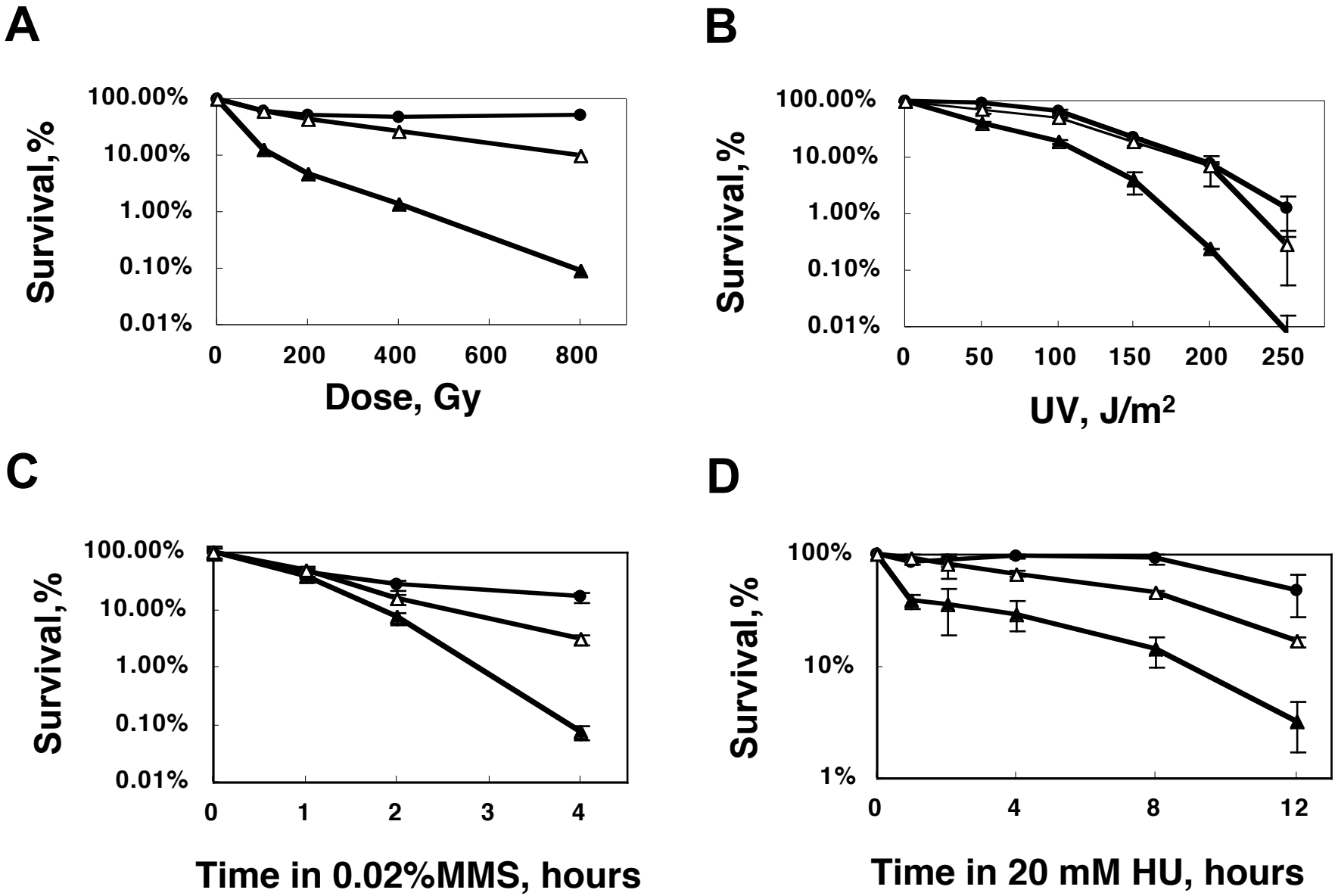
A
Survival,%
100.00%
10.00%
1.00%
0.10%
0.01%
0
200
400
600
800
Dose, Gy
B
Survival,%
100.00%
10.00%
1.00%
0.10%
0.01%
0
50
100
150
200
250
UV, J/m2
C
Survival,%
100.00%
10.00%
1.00%
0.10%
0.01%
0
1
2
3
4
Time in 0.02%MMS, hours
D
Survival,%
100%
10%
1%
0
4
8
12
Time in 20 mM HU, hours

Fig.2

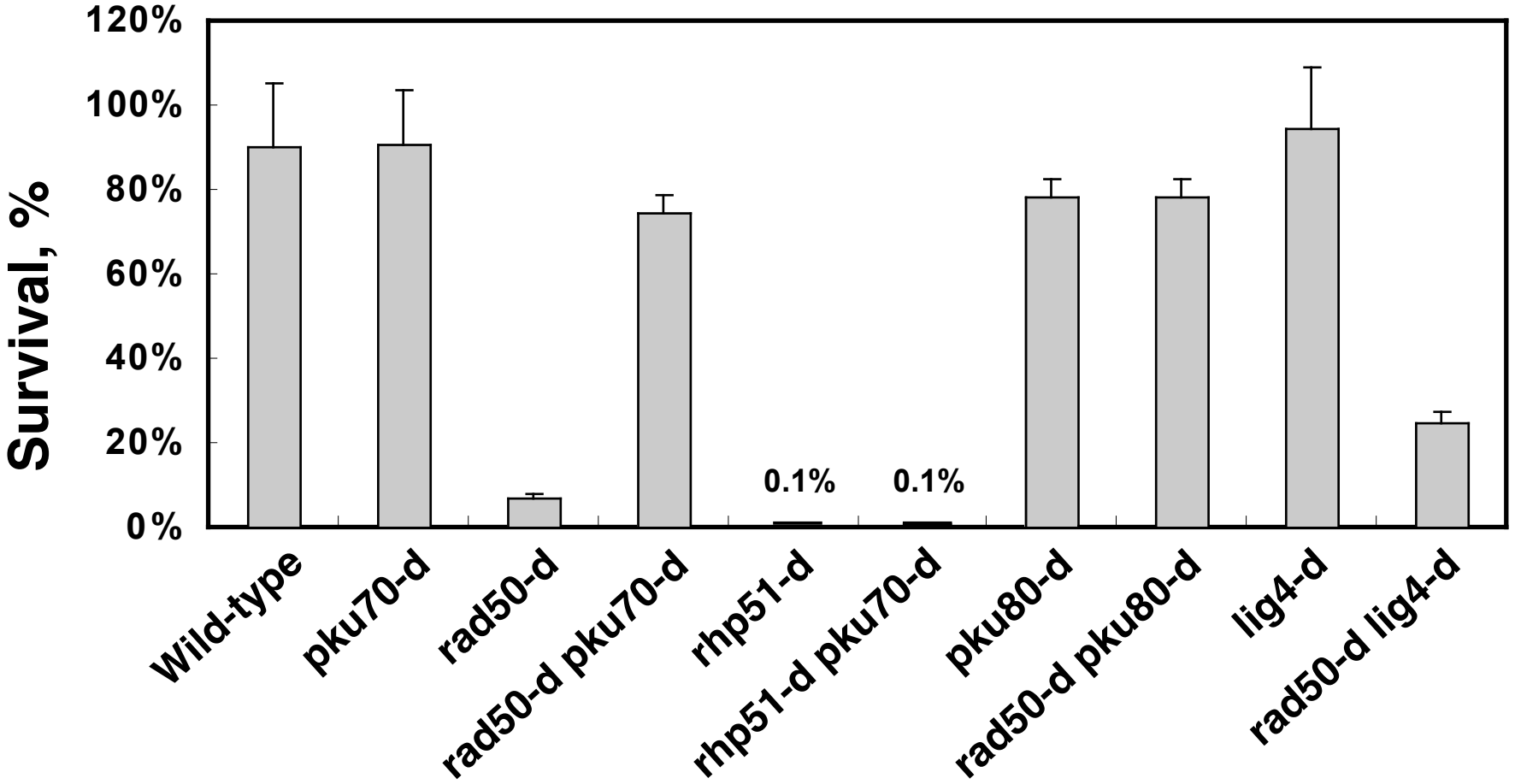
Survival, %
120%
100%
80%
60%
40%
20%
0%
0.1%
0.1%
Wild-type
pku70-d
rad50-d
rad50-d pku70-d
rhp51-d
rhp51-d pku70-d
pku80-d
rad50-d pku80-d
lig4-d
rad50-d lig4-d

Fig.3

A

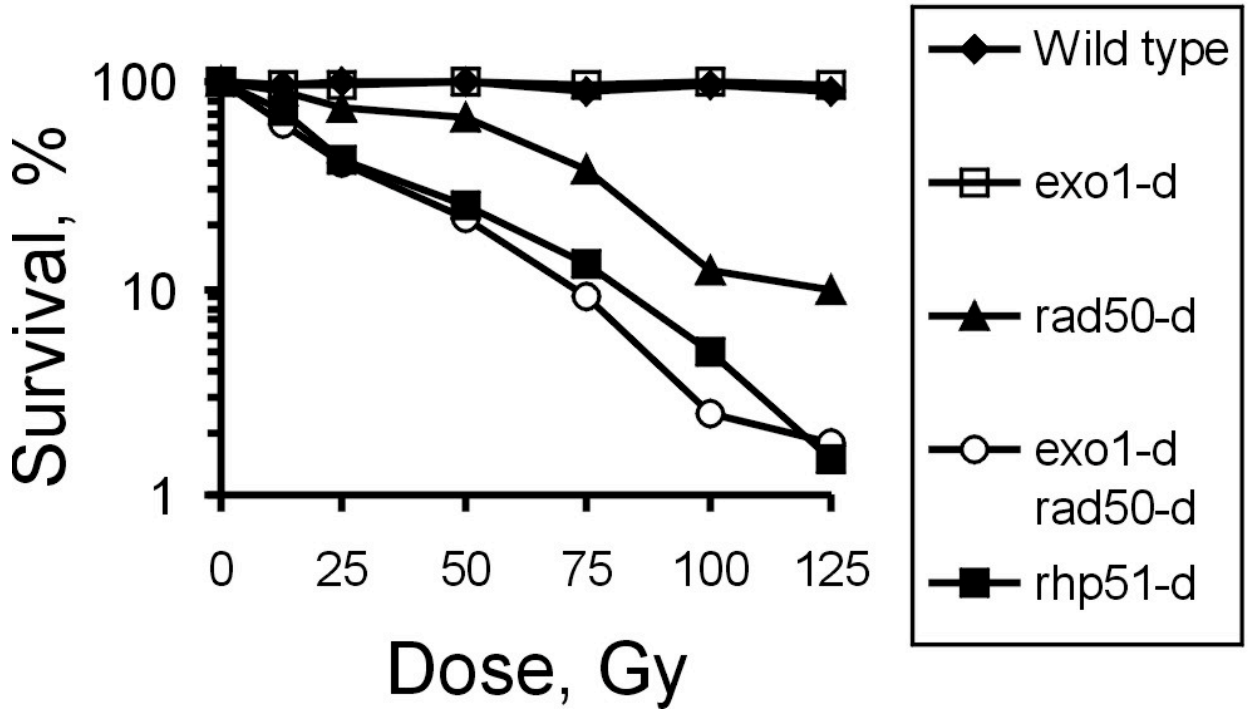
100
10
1
Survival, %
0
25
50
75
100
125
Dose, Gy
Wild type
exo1-d
rad50-d
exo1-d
rad50-d
rhp51-d

B

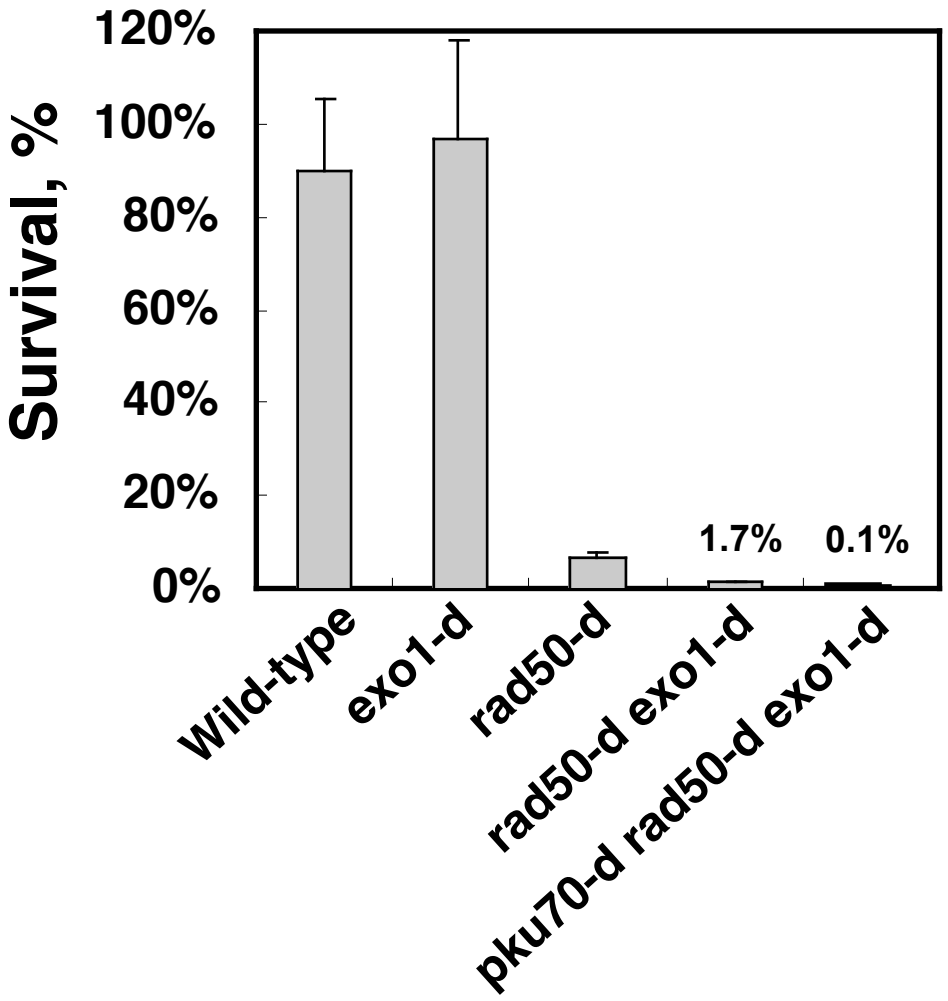
Survival, %
120%
100%
80%
60%
40%
20%
0%
1.7%
0.1%
Wild-type
exo1-d
rad50-d
rad50-d exo1-d
pku70-d rad50-d exo1-d

C

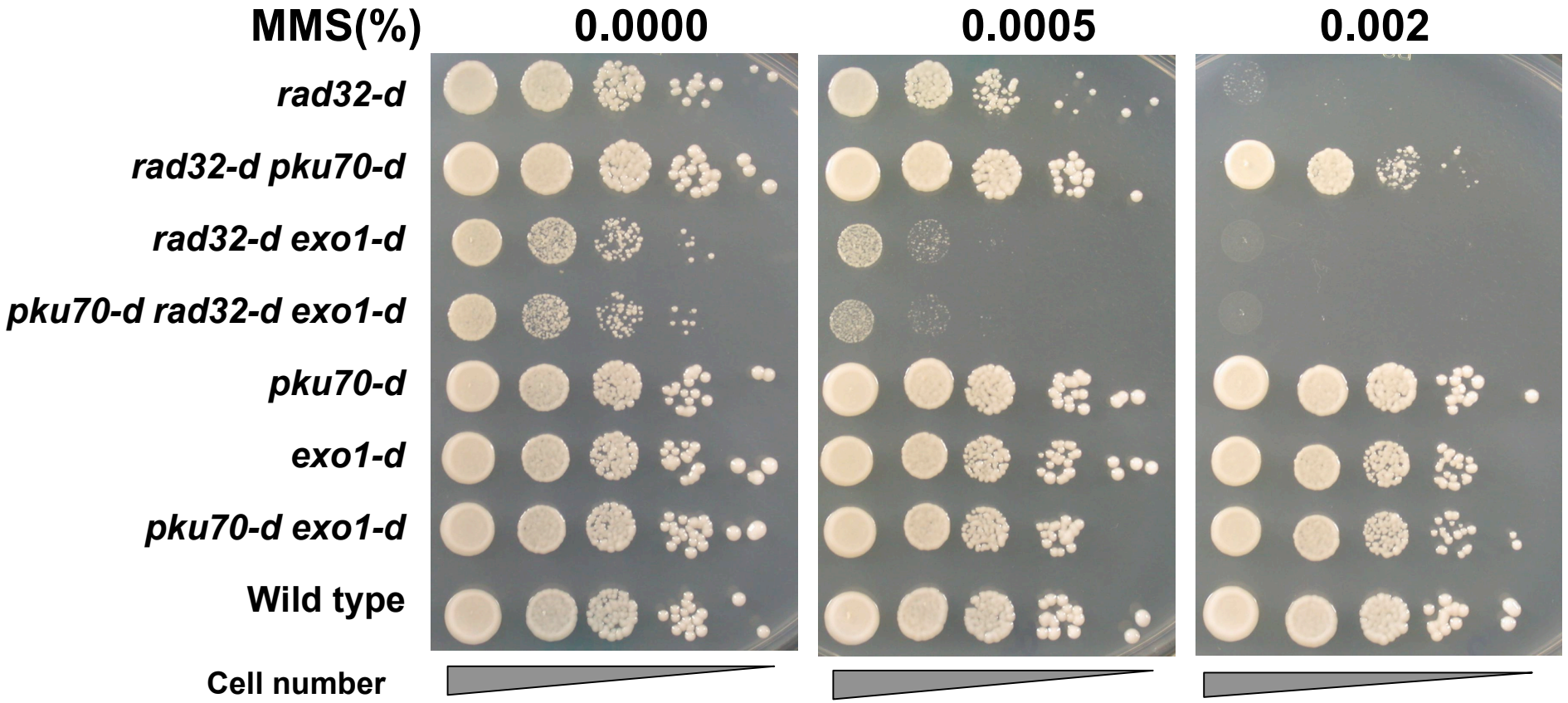
MMS(%)
0.0000
0.0005
0.002
rad32-d
rad32-d pku70-d
rad32-d exo1-d
pku70-d rad32-d exo1-d
pku70-d
exo1-d
pku70-d exo1-d
Wild type
Cell number

Fig.4

A

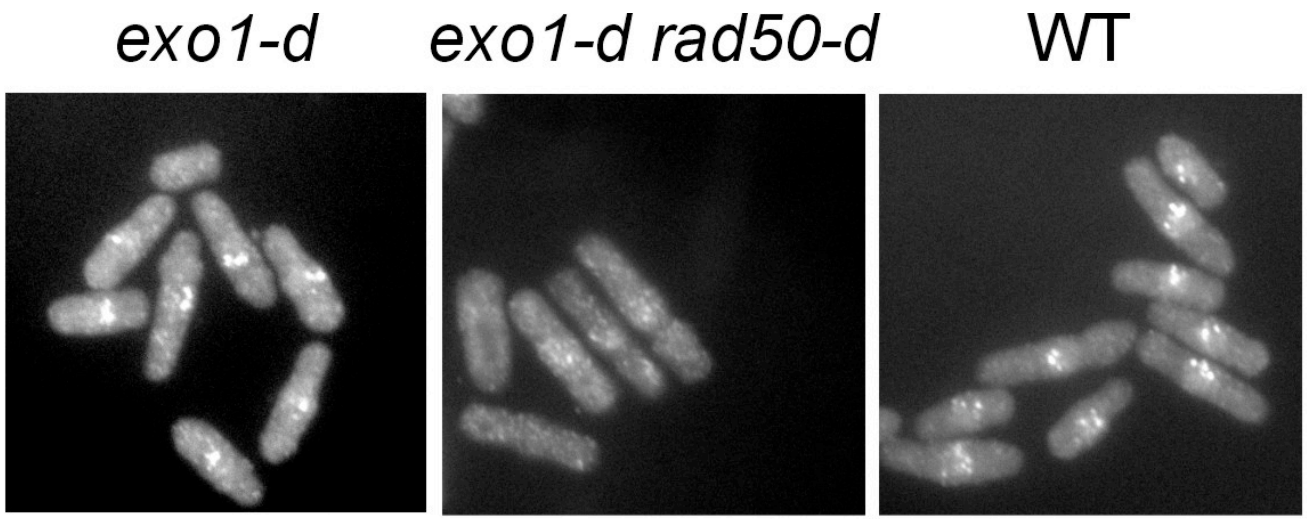
exo1-d
exo1-d rad50-d
WT

B

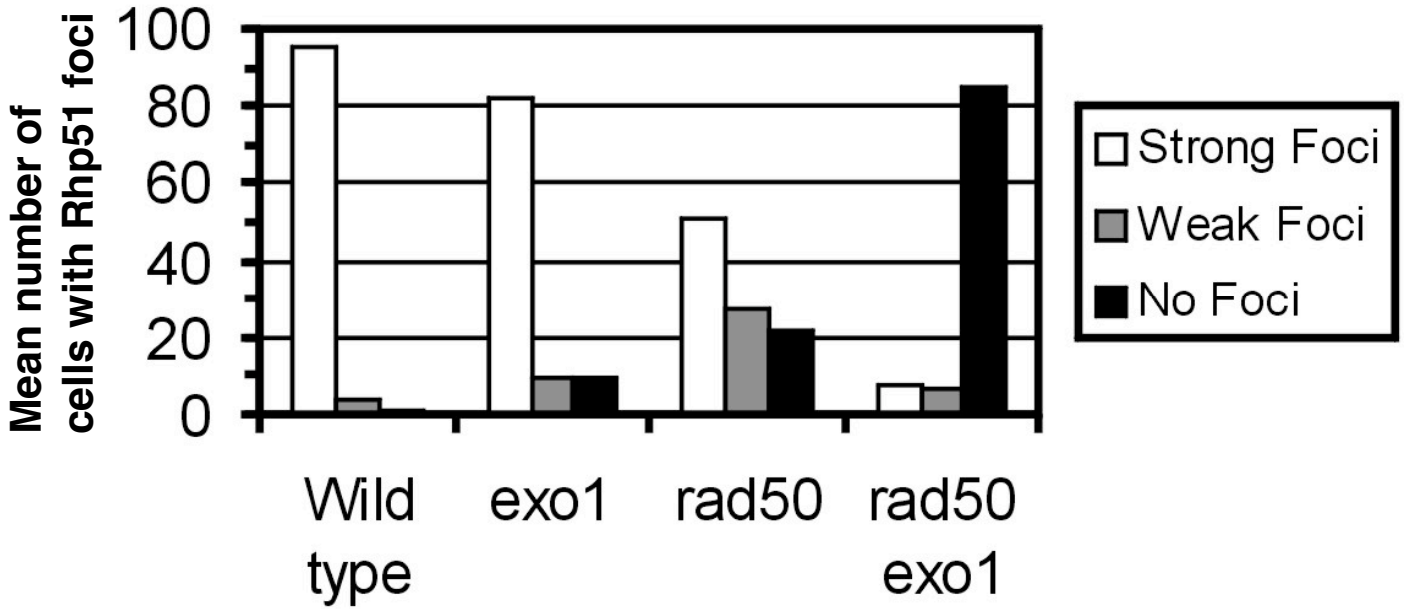
Mean number of cells with Rhp51 foci
100
80
60
40
20
0
Wild type
exo1
rad50
rad50 exo1
Strong Foci
Weak Foci
No Foci

Fig.5

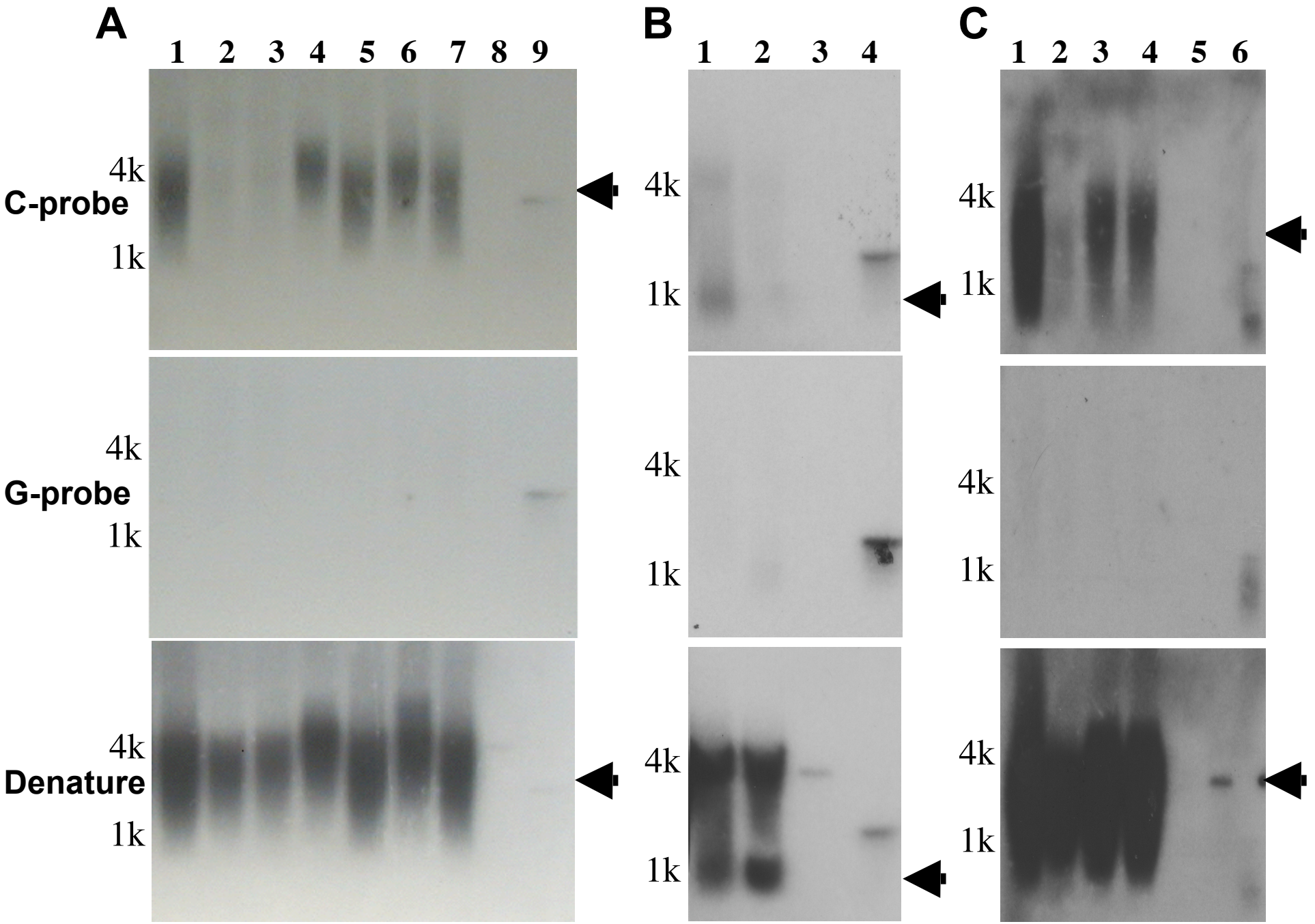
A
1 2 3 4 5 6 7 8 9
4k
C-probe
1k
4k
G-probe
1k
4k
Denature
1k
B
1 2 3 4
4k
1k
4k
1k
4k
1k
C
1 2 3 4 5 6
4k
1k
4k
1k
4k
1k

D

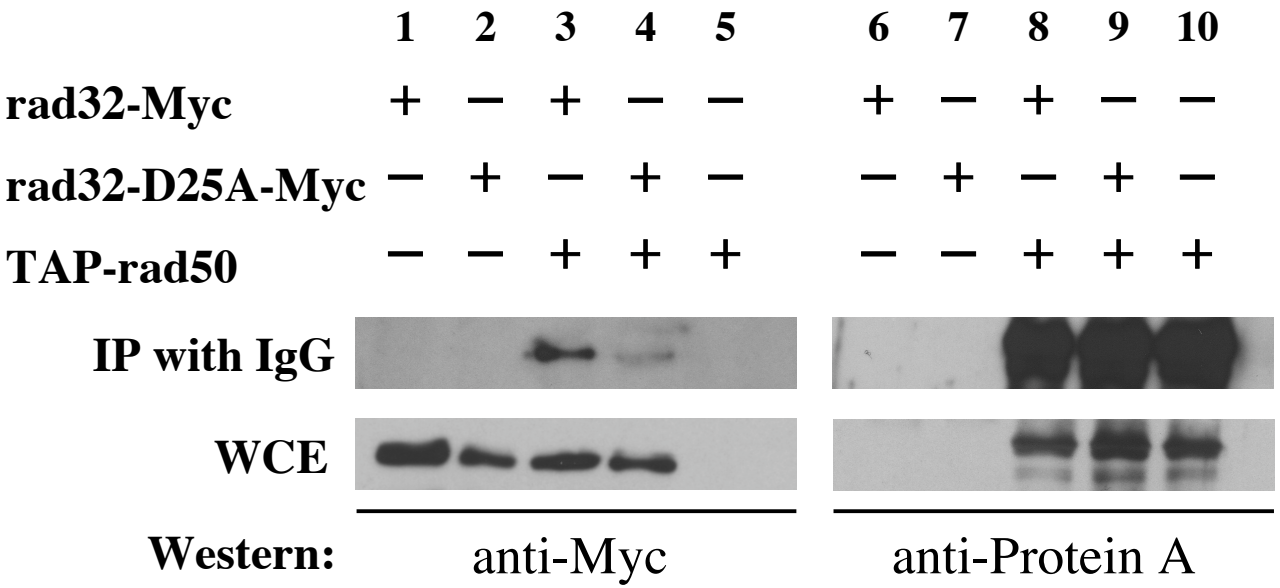
1 2 3 4 5 6 7 8 9 10
rad32-Myc + − + − − + − + − −
rad32-D25A-Myc − + − + − − + − + −
TAP-rad50 − − + + + − − + + +
IP with IgG
WCE
Western:
anti-Myc
anti-Protein A

E

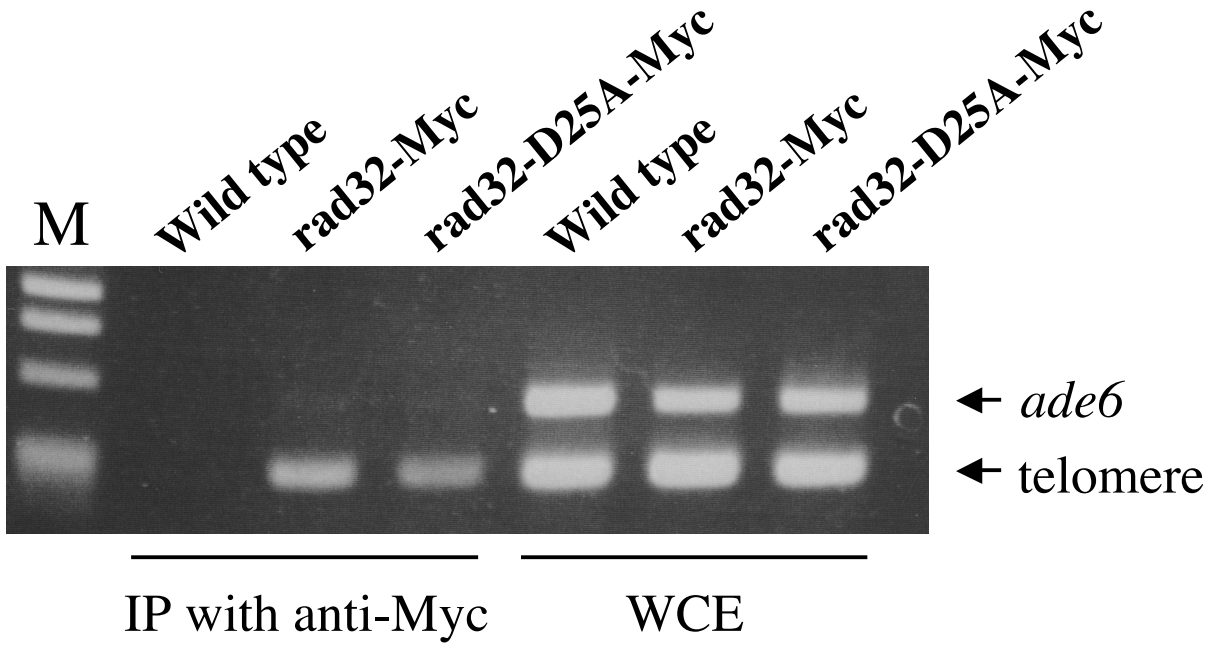
M
Wild type
rad32-Myc
rad32-D25A-Myc
Wild type
rad32-Myc
rad32-D25A-Myc
ade6
telomere
IP with anti-Myc
WCE

Fig.6

A

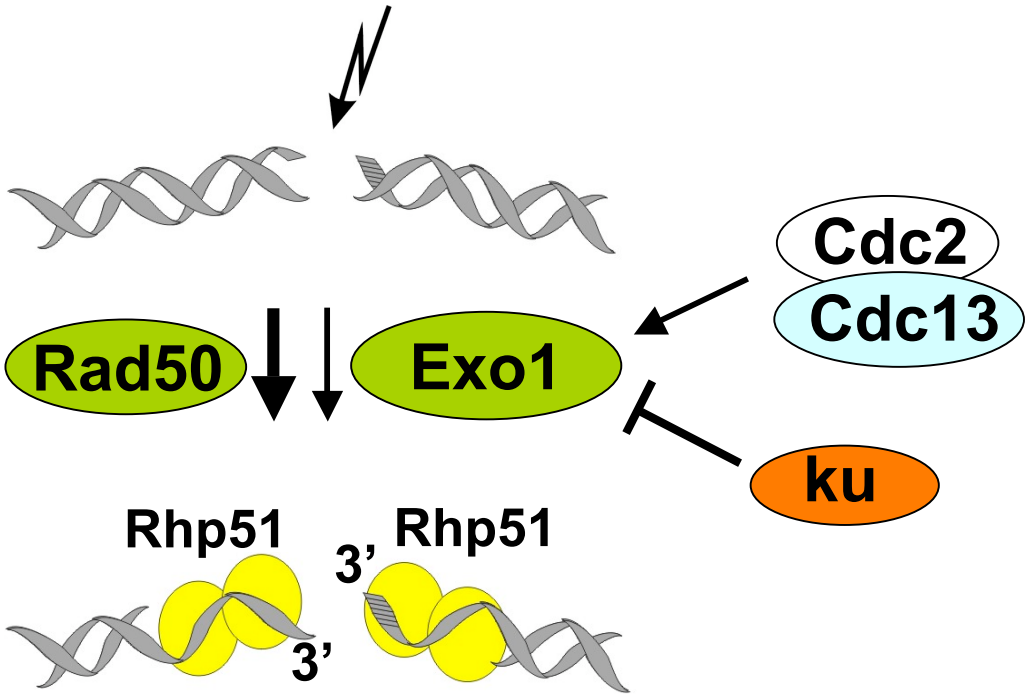
Cdc2
Cdc13
Rad50
Exo1
ku
Rhp51
3’
Rhp51
3’

B

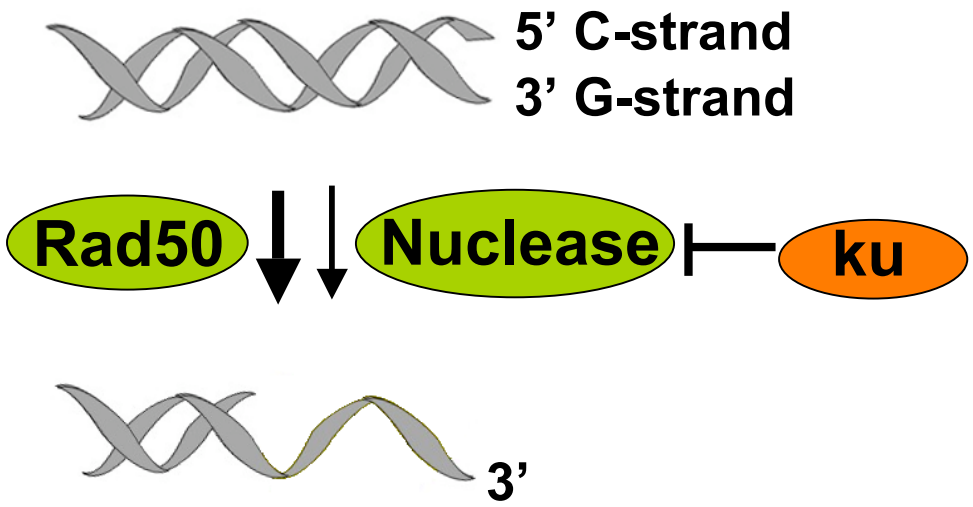
5’ C-strand
3’ G-strand
Rad50
Nuclease
ku
3’